BJP British Journal of Pharmacology

DOI:10.1111/bph.12619
www.brjpharmacol.org

RESEARCH PAPER

Anti-arthritis effects of (E)-2,4-bis(*p*-hydroxyphenyl)-2-butenal are mediated by inhibition of the STAT3 pathway

Jung Ok Ban[1]*, Dae Hwan Kim[1]*, Hee Pom Lee[1], Chul Ju Hwang[1], Jung-Hyun Shim[2], Dae Joong Kim[3], Tae Myoung Kim[3], Heon-Sang Jeong[4], Seong Su Nah[5], Hanyong Chen[6], Zigang Dong[6], Young Wan Ham[7], Youngsoo Kim[1], Sang-Bae Han[1] and Jin Tae Hong[1]

[1]*College of Pharmacy, Medical Research Center, Chungbuk National University, Cheongju, Chungbuk, Korea,* [2]*Natural Medicine Research Institute, Department of Pharmacy, College of Pharmacy, Mokpo National University, Jeonnam, Korea,* [3]*College of Veterinary Medicine, Chungbuk National University, Cheongju, Chungbuk, Korea,* [4]*Agriculture, Life and Environments Sciences, Chungbuk National University, Cheongju, Chungbuk, Korea,* [5]*Division of Rheumatology, Department of Internal Medicine, College of Medicine, Soonchunhyang University, Choenan, Korea,* [6]*Hormel Institute, University of Minnesota, Austin, MN, USA, and* [7]*Department of Chemistry and Biochemistry, Brigham Young University, Provo, UT, USA*

Correspondence
Jin Tae Hong, College of Pharmacy, Medical Research Center, Chungbuk National University, 12 Gaeshin-dong, Heungduk-gu, Cheongju, Chungbuk 361-763, Korea.
E-mail: jinthong@chungbuk.ac.kr

*These authors contributed equally to this article.

Keywords
(E)-2,4-bis(*p*-hydroxyphenyl)-2-butenal; STAT3; NF-κB; arthritis; inflammation

Received
30 September 2013
Revised
16 December 2013
Accepted
28 January 2014

BACKGROUND AND PURPOSE

Products of Maillard reactions between aminoacids and reducing sugars are known to have anti-inflammatory properties. Here we have assessed the anti-arthritis effects of (E)-2,4-bis(*p*-hydroxyphenyl)-2-butenal and its possible mechanisms of action.

EXPERIMENTAL APPROACH

We used cultures of LPS-activated macrophages (RAW264.7 cells) and human synoviocytes from patients with rheumatoid arthritis for *in vitro* assays and the collagen-induced arthritis model in mice. NO generation, iNOS and COX2 expression, and NF-κB/IKK and STAT3 activities were measured *in vitro* and in joint tissues of arthritic mice, along with clinical scores and histopathological assessments. Binding of (E)-2,4-bis(*p*-hydroxyphenyl)-2-butenal to STAT3 was evaluated by a pull-down assay and its binding site was predicted using molecular docking studies with Autodock VINA.

KEY RESULTS

(E)-2,4-bis(*p*-hydroxyphenyl)-2-butenal (2.5–10 μg·mL^{-1}) inhibited LPS-inducedNO generation, iNOS and COX2 expression, and NF-κB/IKK and STAT3 activities in macrophage and human synoviocytes. This compound also suppressedcollagen-induced arthritic responses in mice by inhibiting expression of iNOS and COX2, and NF-κB/IKK and STAT3 activities; it also reduced bone destruction and fibrosis in joint tissues. A pull-down assay showed that (E)-2,4-bis(*p*-hydroxyphenyl)-2-butenal interfered with binding of ATP to STAT3. Docking studies suggested that (E)-2,4-bis(*p*-hydroxyphenyl)-2-butenal bound to the DNA-binding interface of STAT3 possibly inhibiting ATP binding to STAT3 in an allosteric manner.

CONCLUSIONS AND IMPLICATIONS

(E)-2,4-bis(*p*-hydroxyphenyl)-2-butenal exerted anti-inflammatory and anti-arthritic effects through inhibition of the NF-κB/STAT3 pathway by direct binding to STAT3. This compound could be a useful agent for the treatment of arthritic disease.

Abbreviations

CIA, collagen-induced arthritis; CFA, complete Freund's adjuvant; FLS, fibroblast-like synoviocytes; IKKβ, IκB kinase β

Introduction

Reactive oxygen species (ROS) and NO play important physiological roles as mediators of signalling processes. However, the excessive production of endogenous and/or exogenous ROS and NO is implicated in the pathogenesis of inflammatory disease and cancer (Ma, 2010). It is well known that, in rheumatoid arthritis, immune cells participate in the process of the inflammatory or immune response by generating ROS, NO and PGE_2 (Phillips *et al.*, 2010). NF-κB, a redox-sensitive transcription factor, is activated by oxidative stress and inflammatory mediators, and plays a key role in the development of arthritic disease (Okamoto *et al.*, 2010; Morgan and Liu, 2011). The activation of NF-κB is mediated by IκB kinases (IKKs) through oxidative and inflammatory stress (Morgan and Liu, 2011). Thus, NF-κB and/or IKKs may be suitable targets for anti-inflammatory drugs having antioxidant properties. Many recent reports have demonstrated that several antioxidants such as gravinol, phloroglucinol, pycnogenol and curcumin provide anti-inflammatory effects through the inactivation of IKKs and/or NF-κB (Peng *et al.*, 2000; Kowluru and Kanwar, 2007; Kim and Kim, 2010; Kim *et al.*, 2010).

STAT3 is another important transcription factor involved in inflammation and immune responses and it interacts with NF-κB (Grivennikov and Karin, 2010). Hagihara *et al.* (2005) demonstrated that STAT3 forms a complex with the p65 subunit of NF-κB, following stimulation of cells with cytokines and inflammatory mediators. Yu *et al.* (2002) reported a physical and functional interaction between STAT3 and p65 which inhibits the transcriptional activation of the iNOS gene. Activation of STATs is critical in the development of rheumatoid arthritis, and several anti-inflammatory compounds, such as melittin, and moxibustion may inhibit development of rheumatoid arthritis by preventing STAT3 activation (Lo *et al.*, 2005; Yang *et al.*, 2007; Kim *et al.*, 2011). Nowell *et al.* (2009) also reported that STAT3 was critical for IL-6-induced synovial infiltration in inflammatory arthritis. In addition, several reports suggested that STAT3 is crucial for the direct regulation of the expression of oxidant or inflammatory mediators such as NO, iNOS, COX-2, IL-6 and IL-1 (Lo *et al.*, 2005).

The Maillard reaction between aminoacids and reducing sugars, yielding products such as glucose-tyrosine, has been studied most extensively in foods, although it can occur in animals *in vivo* during the formation of advanced glycation endproducts. The Maillard reaction products are known to have anti-oxidant (Valls-Bellés *et al.*, 2004; Yilmaz and Toledo, 2005), anti-mutagenic (Yen *et al.*, 1992) and anticardiogenic activities (Aeschbacher, 1990). The antioxidant capacity of Maillard reaction products is comparable to those of commonly used food antioxidants, such as butylated hydroxyanisole, butylated hydroxytoluene and α-tocopherol (Monti *et al.*, 1999). The Maillard reaction may produce, non-enzymically, coloured or colourless products, such as glucose-tyrosine, glucose-lysine, fructose-lysine, ribose-lysine, xylose-arginine, xylose-glycine and xylose-tryptophan (Aeschbacher, 1990; Valls-Bellés *et al.*, 2004). Recently, we synthesized (E)-2,4-bis(*p*-hydroxyphenyl)-2-butenal using tyrosine and fructose under typical Maillard reaction conditions, including high temperature and pressure (Hwang *et al.*, 2011), and described its antioxidant and anti-inflammatory properties in brain macrophages (Nah *et al.*, 2010; Kim *et al.*, 2013), as well as anti-cancer and anti-amyloidogenic effects through inhibition of the NF-κB and STAT pathways via antioxidant mechanisms (Ban *et al.*, 2009; Jin *et al.*, 2013; Kim *et al.*, 2013). In the present study, we have investigated whether (E)-2,4-bis(*p*-hydroxyphenyl)-2-butenal can provide antioxidant and anti-inflammatory activities, and thus anti-arthritic activities through the inhibition of NF-κB/IKK and STAT3 pathways in a macrophage cell line and in human synoviocytes *in vitro* and in a model of collagen-induced arthritis (CIA) in mice.

Methods

RAW 264.7 cell culture

RAW 264.7, a mouse macrophage-like cell line, was obtained from the American Type Culture Collection (Cryosite, Lane Cove, NSW, Australia). DMEM, penicillin, streptomycin and FBS were purchased from Gibco Life Technologies (Rockville, MD, USA). RAW 264.7 cells were grown in DMEM with 10% FBS, 100 $U \cdot mL^{-1}$ penicillin, and 100 $\mu g \cdot mL^{-1}$ streptomycin at 37°C in 5% CO_2 humidified air.

Human synoviocyte culture

The Clinical Research Ethics Committee of College of Medicine, Soonchunhyang University Medical Center, approved the study protocol and the use of human tissues. Informed consent was obtained from all patients. Patients with rheumatoid arthritis were diagnosed according to the 1987 Revised Criteria of the American College of Rheumatology. Synovial tissue samples were obtained from patients with long-standing rheumatoid arthritis [12 males, 3 females; age 65 ± 21.3 years (mean ± SD); mean disease duration ≥10 years] at the time of total knee joint replacement. Human fibroblast-like synoviocytes (FLSs) were cultured as previously described (Nah *et al.*, 2010). In brief, FLSs were propagated in culture dishes (Nalge Nunc International, Rochester, NY, USA) in DMEM medium (Gibco Life Technologies) supplemented with 20% heat-inactivated FBS (Gibco Life Technologies) and 50 $U \cdot mL^{-1}$ penicillin/streptomycin. All cultures and incubations were carried out in a CO_2 incubator at 37°C in an atmosphere of 5% CO_2. Medium was changed every 3 days. Cells were used between the fifth and the tenth passages. The same cultures were used for each experiment. For experiments, FLSs were detached using trypsin and transferred to 6-well plates (Iwaki, Funabasi, Chiba, Japan).

Cell viability assay

To determine the cell number, cells were plated onto 24-well plates (5×10^4 cells per well). The cells were then trypsinized, pelleted by centrifugation for 5 min at 250× *g* and resuspended in 10 mL of PBS. Next, 0.1 mL of 0.2% Trypan blue was added to the cell suspension in each of the solutions (0.9 mL each). Subsequently, a drop of suspension was placed into a Neubauer chamber (Blaubrand, Wertheim, Germany), and the living, unstained, cells were counted. Each assay was carried out in triplicate.

Nitrite assay

RAW 264.7 cells were plated at 1×10^4 cells per well in 96-well plates and subsequently incubated with or without LPS (1 μg·mL^{-1}) in the absence or presence of various concentrations of (E)-2,4-bis(*p*-hydroxyphenyl)-2-butenal for 24 h. The nitrite in the supernatant was assessed using a NO detection kit purchased from iNtRON Biotechnology (Seongnam, Korea), according to the manufacturer's instructions.

ROS analysis

The level of ROS was measured as described previously (Kim *et al.*, 2013).

PGE_2 analysis

Samples of cell media were analysed for PGE_2 with kits purchased from R&D Systems (Minneapolis, MN, USA) according to the manufacturer's instructions.

EMSA

EMSA was performed as described previously (Kim *et al.*, 2013). The relative density of the protein bands was scanned for densitometry using MyImage and quantified by Labworks 4.0 software (UVP, Inc., Upland, CA, USA).

Transfection and luciferase assay

Transfection and luciferase assays were performed as described previously (Kim *et al.*, 2013).

Western blot analysis

Western blot analysis was performed as described previously (Kim *et al.*, 2013). The membrane was incubated with the following antibodies: mouse polyclonal antibodies against p50, p-IκB, histone H1 and β-actin (1:500 dilution, Santa Cruz Biotechnology Inc., Santa Cruz, CA, USA), rabbit polyclonal antibodies against p65 and IκB (1:500 dilution, Santa Cruz Biotechnology Inc.), and iNOS and COX-2 (1:1000 dilution, Cayman Chemical, Ann Arbor, MI, USA). The relative density of the protein bands was scanned for densitometry using MyImage and quantified by Labworks 4.0 software (UVP, Inc.).

Immunoprecipitation and kinase assays

Whole cell lysates and tissue homogenates were prepared with immunoprecipitation lysis buffer [20 mM HEPES, pH 7.4, 150 mM NaCl, 1.5 mM EDTA, 1% phosphatase and 1% protease inhibitor cocktail (Sigma-Aldrich Corp, St Louis, MO, USA)] and kept on ice for 20 min before centrifugation (16,000× *g*; 12 min, 4°C). The IKK complex was immunoprecipitated by incubation for 12 h at 4°C with the polyclonal IKKα or IKKβ antibody bound to protein A/G PLUS agarose (Santa Cruz Biotechnology Inc.). The immunoprecipitates were washed twice with kinase buffer (20 mM HEPES, pH 7.4, 10 mM $MgCl_2$, 2 mM DTT, 5 mM β-glycerophosphate, 0.1 mM sodium orthovanadate). The kinase assays were initiated by the addition of 2 μg GST-IκBα fusion protein as the substrate and 0.5 μCi [γ-^{32}P]ATP. The reactions were incubated for 30 min at 30°C and stopped by the addition of 5 × SDS-PAGE sample buffer. Phosphorylation of the IκBα proteins was measured by SDS-PAGE followed by autoradiography and densitometry.

Quantitative real-time PCR

Real-time PCR was performed as described previously (Kim *et al.*, 2013).

Induction and assessment of CIA

All animal care and experimental procedures complied with the Korea Food and Drug Administration guidelines as well as the regulations for the care and use of laboratory animals of the Animal Ethics Committee of Chungbuk National University (CBNUA-023-0902-01) who also approved this project. All studies involving animals are reported in accordance with the ARRIVE guidelines for reporting experiments involving animals (Kilkenny *et al.*, 2010; McGrath *et al.*, 2010). A total of 40 animals were used in the experiments described here. Six-week-old male DBA/J1 mice were purchased from Japan SLC, Inc. (Shizuoka, Japan). Bovine collagen type II (Chondrex, Inc., Redmond, WA, USA) was mixed with complete Freund's adjuvant (CFA) (Chondrex, Inc.) and injected intradermally on day 0 at the base of the tail of 8- to 11-week-old mice (100 μg collagen type II and 100 μg CFA in a total volume of 100 μL emulsion). On day 20, the mice received an i.p. booster injection with 100 μg of collagen type II in PBS. After the boosting, the mice were given (E)-2,4-bis(*p*-hydroxyphenyl)-2-butenal (5 mg·kg^{-1}, p.o.), dissolved in 100 μL PBS containing 0.5 μL DMSO, vehicle (negative control) or indomethacin (5 mg·kg^{-1}, p.o.), dissolved in 100 μL PBS, once daily for 30 days. The mice were weighed twice per week. The changes in body weights between the control and the (E)-2,4-bis(*p*-hydroxyphenyl)-2-butenal-treated mice ($n = 10$ for each group) were not significantly different (data not shown). The severity of the arthritis was assessed using a semi-quantitative scoring system (0–4): 0, normal; 1, redness and/or swelling in one joint; 2, redness and/or swelling in more than one joint; 3, redness and/or swelling in the entire paw; 4, deformity and/or ankylosis (Jin *et al.*, 2013). The total score is 16 for each mouse by adding up the scores from all four paws.

Immunohistochemistry (IHC)

IHC was performed as described previously (Kim *et al.*, 2013).

Complete blood count test

The total white blood cell (WBC) and lymphocyte (LYM) counts were measured by an HIE cell counter (Technicon Instruments, Miles Laboratories, Tarrytown, NY, USA) using heparinized blood drawn at day 30.

Splenocyte NO assay

Immediately after killing, spleens were removed, minced into small pieces, and passed through a tissue sieve (200 mesh per 2.5 cm) to prepare single cell suspensions in PBS. The suspension was centrifuged at 250× *g*. for 4 min and the supernatant was discarded. The precipitate was washed with PBS three times and suspended in 2 mL RPMI 1640 complete media. Viable cells were detected by Trypan blue dye exclusion. The

cell density was counted and adjusted to 3×10^6 cells mL^{-1}. Samples of 3×10^6 cells were suspended in RPMI 1640 with ConA (5 $\mu g \cdot mL^{-1}$) and incubated at 37°C with 5% CO_2. After 48 h, the cells were suspended in RPMI 1640 with methyl-α-D-pyranoside (10 $mg \cdot mL^{-1}$) for 30 min. The cells were collected and washed with PBS three times. 1×10^6 cells were suspended in 1 mL RPMI 1640 with IL-2 (10 $pg \cdot mL^{-1}$) and incubated at 37°C with 5% CO_2 for 24 h. Nitrite was assayed as described above.

Molecular modelling

Docking studies were performed between STAT3 and 2,4-bis(*p*-hydroxyphenyl)butenal (Trott and Olson, 2010). The model of STAT3 was obtained from the X-ray crystal structure of dimeric unphosphorylated STAT3 core fragment (PDB ID: 3CWG) (Ren *et al.*, 2008). Only one monomer of the homodimeric STAT3 crystal structure was used in the docking experiments and conditioned using AutodockTools by adding all polar hydrogen atoms. Three dimensional structure of 2,4-bis(*p*-hydroxyphenyl)butenal was built using ChemBio3D and Discovery Studio 3.5 Client, which was further prepared using AutodockTools to rotate during the molecular simulation through all eight rotatable single bonds. The grid box was centred on the STAT3 monomer and the size of the grid box was adjusted to include the whole monomer. Docking experiments were performed at various exhaustiveness values of the default: 16, 24, 32, 40 and 60. Molecular graphics for the best binding model was generated using Discovery Studio Visualizer 2.0.

Data analysis

Data were expressed as mean ± SD. Data were analysed using the Shapiro–Wilk normality test and one-way ANOVA was used for comparison between groups, followed by *post hoc* Tukey test (SPSS version 18.0; SPSS Inc., Chicago, IL, USA). $P < 0.05$ showed statistical significance.

Materials

The characterization of (E)-2,4-bis(*p*-hydroxyphenyl)-2-butenal has been described previously (Hwang *et al.*, 2011) and its chemical structure is shown in Figure 7A. (E)-2,4-bis(*p*-hydroxyphenyl)-2-butenal was dissolved in 0.05% DMSO and the cultured cells were treated with concentrations of 2.5, 5 and 10 $\mu g \cdot mL^{-1}$. LPS, TNF-α and indomethacin were purchased from Sigma-Aldrich Co.

Results

Inhibitory effect of (E)-2,4-bis(p-hydroxyphenyl)-2-butenal on LPS-induced ROS, NO and PGE_2 generation, and the expression of iNOS and COX-2 in RAW 264.7 cells

After co-treatment of RAW 264.7 cells with LPS (1 $\mu g \cdot mL^{-1}$) and (E)-2,4-bis(*p*-hydroxyphenyl)-2-butenal (0–10 $\mu g \cdot mL^{-1}$), the production of the LPS-induced ROS, NO and PGE_2 was decreased in a concentration-dependent manner (Figure 1A–C). In addition, we assessed the effects of (E)-2,4-bis(*p*-hydroxyphenyl)-2-butenal on expression of the corresponding genes controlling NO and PGE_2 production. It inhibited both LPS-induced iNOS-luciferase activity and expression of iNOS and COX-2 in a concentration-dependent manner (Figure 1D, E). However, the cell viability of LPS-induced RAW 264.7 cells was not affected up to a concentration of 10 $\mu g \cdot mL^{-1}$ (Figure 1F), suggesting that the compound was not cytotoxic at the levels used here.

Inhibitory effect of (E)-2,4-bis(p-hydroxyphenyl)-2-butenal on NF-κB, IKK and STAT3 activities and the expression level of pro-inflammatory cytokines

First, we studied whether (E)-2,4-bis(*p*-hydroxyphenyl)-2-butenal inhibits NF-κB activity leading to the inhibition of iNOS and COX-2 expression in RAW 264.7 cells. LPS induced a strong NF-κB DNA-binding activity, transcriptional activity, the nuclear translocation of NF-κB subunits p65 and p50, and degradation of IκB (increased phosphorylation), all of which were attenuated in a concentration-dependent manner by co-treatment of the cells with (E)-2,4-bis(*p*-hydroxyphenyl)-2-butenal (Figure 2A–C). The NF-κB DNA-binding activity was confirmed with competition and supershift assays (data not shown). Because IκB is phosphorylated by activated IKKs in the classical pathway, we examined whether (E)-2,4-bis(*p*-hydroxyphenyl)-2-butenal inhibited IKK activity, by monitoring the phosphorylation of IKK as well as its kinase activity. (E)-2,4-bis(*p*-hydroxyphenyl)-2-butenal inhibited LPS-induced phosphorylation of both IKKα and IKKβ (Figure 2D, upper panel). However, it reduced the kinase activity of the LPS-induced IKKβ (Figure 2D, lower panel).

STAT3 is another important redox transcription factor involved in the inflammation and immune responses, and it interacts with NF-κB (Hagihara *et al.*, 2005; Kim *et al.*, 2011). In RAW 264.7 cells, (E)-2,4-bis(*p*-hydroxyphenyl)-2-butenal inhibited LPS-induced STAT3 DNA-binding activity and phosphorylation (Figure 3A, B). Consequently, it inhibited the LPS-induced increase in IL-6, IL-1β and TNF-α mRNA expression in a concentration-dependent manner (Figure 3C).

To further study this inhibition of STAT3-mediated NF-κB activity and inflammatory responses, we examined the effect of STAT3 inhibition using a STAT3 inhibitor (Stattic; Sigma-Aldrich) or an STAT3 siRNA. Treatment with Stattic at a concentration of 1 μM or 200 pmol STAT3 siRNA abolished the inhibitory effect of (E)-2,4-bis(*p*-hydroxyphenyl)-2-butenal on NF-κB (Figure 3D). Co-treatment of STAT3 inhibitor Stattic or STAT3 siRNA with LPS and (E)-2,4-bis(*p*-hydroxyphenyl)-2-butenal also attenuated the inhibitory effect of the compound on NO generation as well as cytokine mRNA levels (Figure 3E, F). These data demonstrate possible interactions between STAT3 and NF-κB in terms of their anti-inflammatory effects.

In addition, we studied whether (E)-2,4-bis(*p*-hydroxyphenyl)-2-butenal could inhibit LPS or TNF-α-induced NO production, and STAT3 and IKKβ/NF-κB activities in human synoviocytes. After co-treatment of LPS (1 $\mu g \cdot mL^{-1}$) or TNF-α (10 ng/mL) with (E)-2,4-bis(*p*-hydroxyphenyl)-2-butenal (10 $\mu g \cdot mL^{-1}$) for 24 h, both LPS

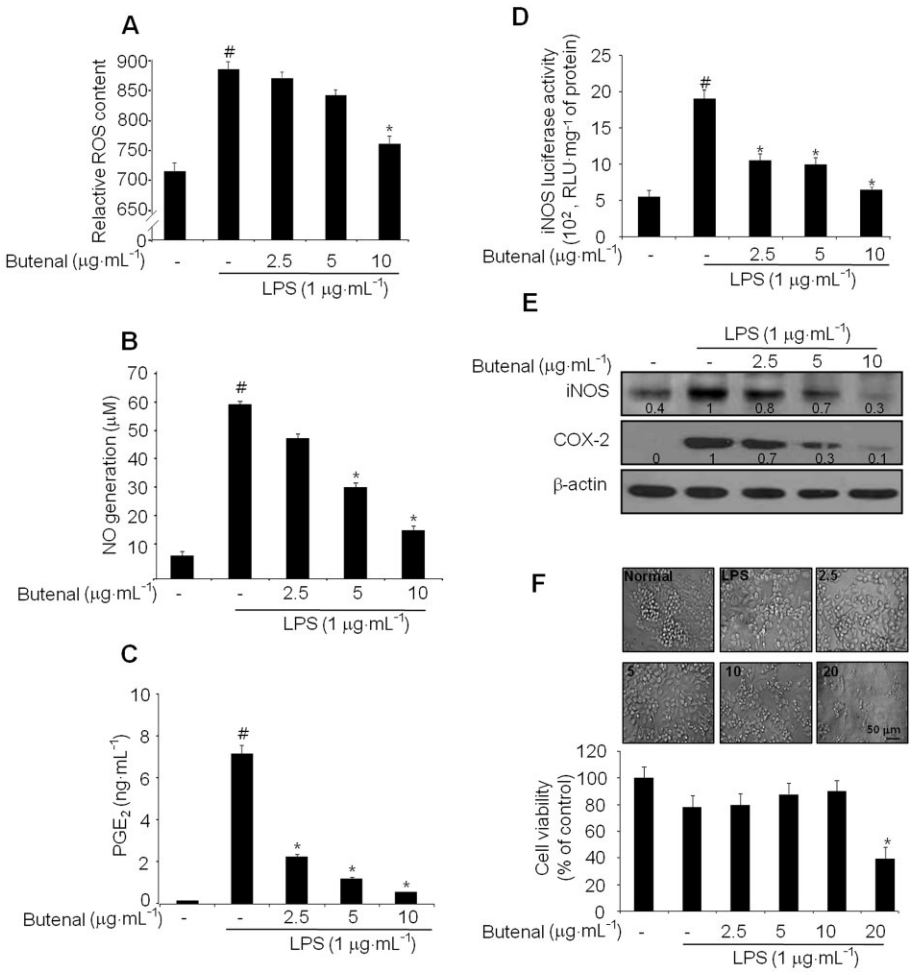

Figure 1

Inhibitory effects of (E)-2,4-bis(*p*-hydroxyphenyl)-2-butenal on LPS-induced ROS, NO and PGE_2 generation, expression of iNOS and COX-2 and cell viability in RAW 264.7 cells. RAW 264.7 cells were treated with 1 μg·mL^{-1} LPS only or LPS combined with a range of concentrations (2.5, 5, 10 μg·mL^{-1}) of (E)-2,4-bis(*p*-hydroxyphenyl)-2-butenal at 37°C for 15 min (for determination of ROS generation) or 24 h (for determination of NO and PGE_2 generation). (A) ROS, (B) NO and (C) PGE_2 generation was determined in culture medium. (D) RAW 264.7 cells were transiently transfected with an iNOS-luciferase construct and activated with LPS (1 μg·mL^{-1}) alone or LPS combined with the indicated concentrations of (E)-2,4-bis(*p*-hydroxyphenyl)-2-butenal for 8 h. Subsequently, luciferase activity was determined. (E) Equal amounts of total protein (40 μg per lane) from 24 h cultured cells were analysed by 10% SDS-PAGE, and the expression of iNOS and COX-2 was detected by Western blotting using specific antibodies. The β-actin protein was used as an internal control. (F) Morphological changes were observed by light microscopy. Cell viability was determined using the Trypan blue assay. All values represent the means ± SD of three independent experiments performed in triplicate. $^{\#}P < 0.05$, significantly different from control group: $^{*}P < 0.05$, significantly different from the LPS-treated group.

and TNF-α-induced NO production were inhibited (Figure 4A, upper panel). However, (E)-2,4-bis(*p*-hydroxyphenyl)-2-butenal (10 μg·mL^{-1}) did not affect cell viability in LPS or TNF-α-induced synoviocytes (Figure 4A, lower panel), showing that the inhibition of NO production was not due to cytotoxicity. Consistent with its inhibitory effect in RAW264.7 cells, (E)-2,4-bis(*p*-hydroxyphenyl)-2-butenal also inhibited STAT3 DNA-binding activity as well as phosphorylation of STAT3 in human synoviocytes (Figure 4B, C). (E)-2,4-bis(*p*-hydroxyphenyl)-2-butenal also inhibited NF-κB DNA-binding activity (Figure 4D) as well as IKKβ phosphorylation (Figure 4E, upper panel) and activity (Figure 4E, lower panel), and phosphorylation of Akt (Figure 4C).

Inhibitory effects of (E)-2,4-bis(p-hydroxyphenyl)-2-butenal on collagen-induced inflammation and arthritis, and the expression of related inflammatory genes

We then determined the anti-arthritic effect of this compound in the mouse model of CIA. (E)-2,4-bis(*p*-hydroxyphenyl)-2-butenal (5 mg·kg^{-1}, p.o.), vehicle (negative control) or indomethacin (5 mg·kg^{-1}, p.o.) was given daily to 6-week-old male DBA/J1 mice for 30 days (Figure 5A). In all groups, the symptoms were not observed prior to the second injection of type II collagen. Mice have signs of disease approximately 6 days after the second collagen (100 μg)

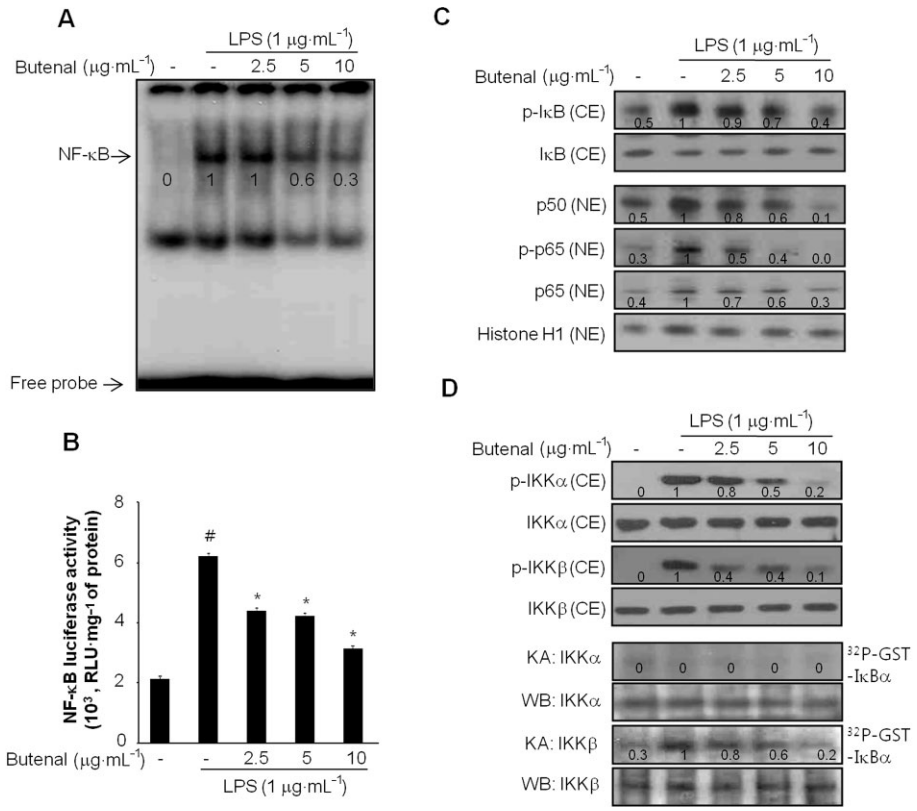

Figure 2

Inhibitory effects of (E)-2,4-bis(*p*-hydroxyphenyl)-2-butenal on LPS-induced IKK/NF-κB activation in RAW 264.7 cells. (A) After treatment with LPS and/or (E)-2,4-bis(*p*-hydroxyphenyl)-2-butenal for 30 min, the DNA-binding activity of NF-κB was investigated using EMSA. (B) RAW 264.7 cells were transfected with p-NF-κB-Luc plasmid (5 × NF-κB) and treated for 8 h. The luciferase activity was then determined. All values represent the means ± SD of three independent experiments performed in triplicate. $^{\#}P < 0.05$, significantly different from control group: $^{*}P < 0.05$, significantly different from the LPS-treated group. (C) Equal amounts of total protein (40 μg) were analysed by 10% SDS-PAGE. Nuclear translocation of p50 and p65 and the degradation of IκB were detected by Western blotting. β-Actin or histone H1 protein was used as an internal control. (D) The expression of IKKα/β (upper panels) was detected by Western blotting (WB) in the cells treated for 15 min. For the IKKα/β kinase assay (KA; lower panels), the IKK complex was immunoprecipitated with an anti-IKK antibody and the *in vitro* kinase assay utilized 2 μM GST-IκBα fusion protein and 5 μCi [γ-^{32}p]ATP. After SDS-PAGE, the phosphorylated IκBα protein was visualized by autoradiography. The values (A, C and D) under the band indicate fold difference (average) from untreated control group.

injection in the arthritis-induced group, but we observed a delay in the onset of CIA symptoms upon treatment with (E)-2,4-bis(*p*-hydroxyphenyl)-2-butenal. On the final treatment day (day 30), the clinical score (about 6) was approximately 51% lower in the group that was treated with (E)-2,4-bis(*p*-hydroxyphenyl)-2-butenal (5 mg·kg^{-1}) than in the CIA group (score about 12), and 49% in the indomethacin-treated (5 mg·kg^{-1}) group. (Figure 5B). A radiographic examination of the hind paws revealed tissue swelling and bone destruction in the paws of collagen-injected mice. However, these effects were markedly reduced by (E)-2,4-bis(*p*-hydroxyphenyl)-2-butenal and its inhibitory effect was comparable with that of indomethacin (Figure 5B). Histopathological evaluation of the ankle joint sections of mice with CIA revealed partial bone destruction (pannus) and fibrosis. In contrast, the extent of bone destruction and fibrosis was significantly reduced in CIA mice treated with (E)-2,4-bis(*p*-hydroxyphenyl)-2-butenal (Figure 5C). Immunohistochemical analysis of ankle joint tissue obtained from CIA mice exhibited markedly positive staining for iNOS and TNF-α, which were localized primarily in fibrous tissue structures surrounding the joints. Treatment with (E)-2,4-bis(*p*-hydroxyphenyl)-2-butenal markedly decreased these positively stained areas (Figure 5C).

As rheumatoid arthritis alters blood cell counts, we measured circulating leukocytes in mice with CIA. Both total leukocytes (WBC) and lymphocytes were higher in CIA mice than in normal mice (Figure 5D) Treatment with either (E)-2,4-bis(*p*-hydroxyphenyl)-2-butenal or indomethacin resulted in a fourfold decrease in the number of total WBC and lymphocytes, compared with those in untreated CIA mice (Figure 5D). In addition, NO generation in splenic T-cells from CIA mice was higher than that from control normal mice and either (E)-2,4-bis(*p*-hydroxyphenyl)-2-butenal or indomethacin decreased this CIA-induced NO production (Figure 5E). (E)-2,4-bis(*p*-hydroxyphenyl)-2-butenal did not affect the progression of body weight or induce any behavioural modifications (data not shown), suggesting that there was no gross *in vivo* toxicity at the dose given. These inhibitory effects were accompanied with the

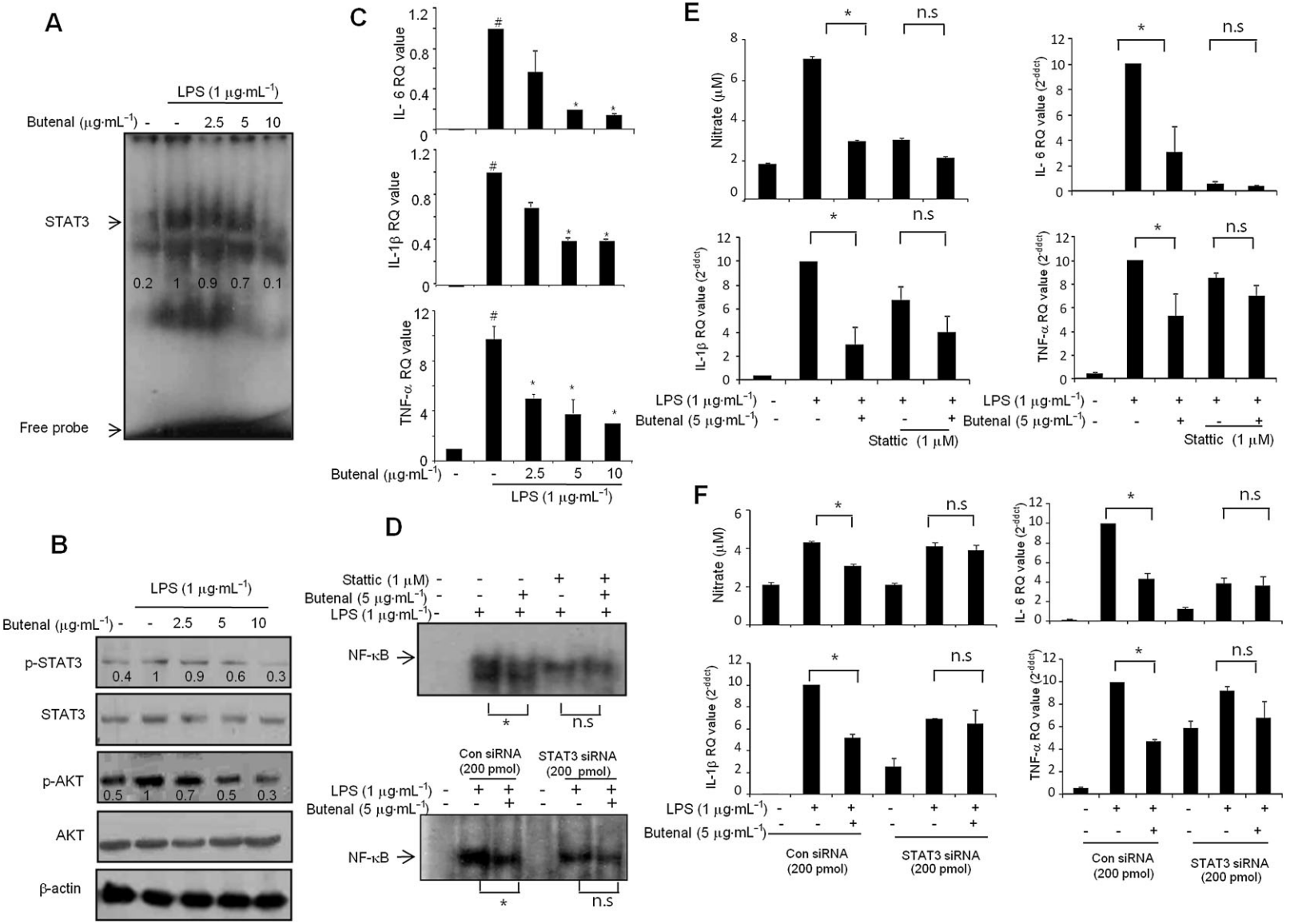

Figure 3

Inhibitory effect of (E)-2,4-bis(*p*-hydroxyphenyl)-2-butenal on LPS-induced STAT3 activation and inflammatory cytokine mRNA expression level and abolished effects of STAT inhibition in RAW 264.7 cells. In (A) data for the DNA-binding activity and in (B) data for expression of STAT3 are shown. (C) Real-time PCR was subsequently performed. $^{\#}P < 0.05$, significantly different from control group: $^{*}P < 0.05$, significantly different from the LPS-treated group. Cells were treated with 1 μM STAT3 inhibitor (Stattic) or 200 pmol STAT3 siRNA in the presence or absence of 5 μg·mL^{-1} (E)-2,4-bis(*p*-hydroxyphenyl)-2-butenal in LPS-induced RAW 264.7 cells. (D) DNA-binding activity, NO generation, as well as the (E, F) mRNA level of IL-6, IL-1β and TNF-α were determined as described in Methods section. All values represent the means ± SD of three independent experiments performed in triplicate. $^{*}P < 0.05$, significantly different as indicated; NS indicates no difference.

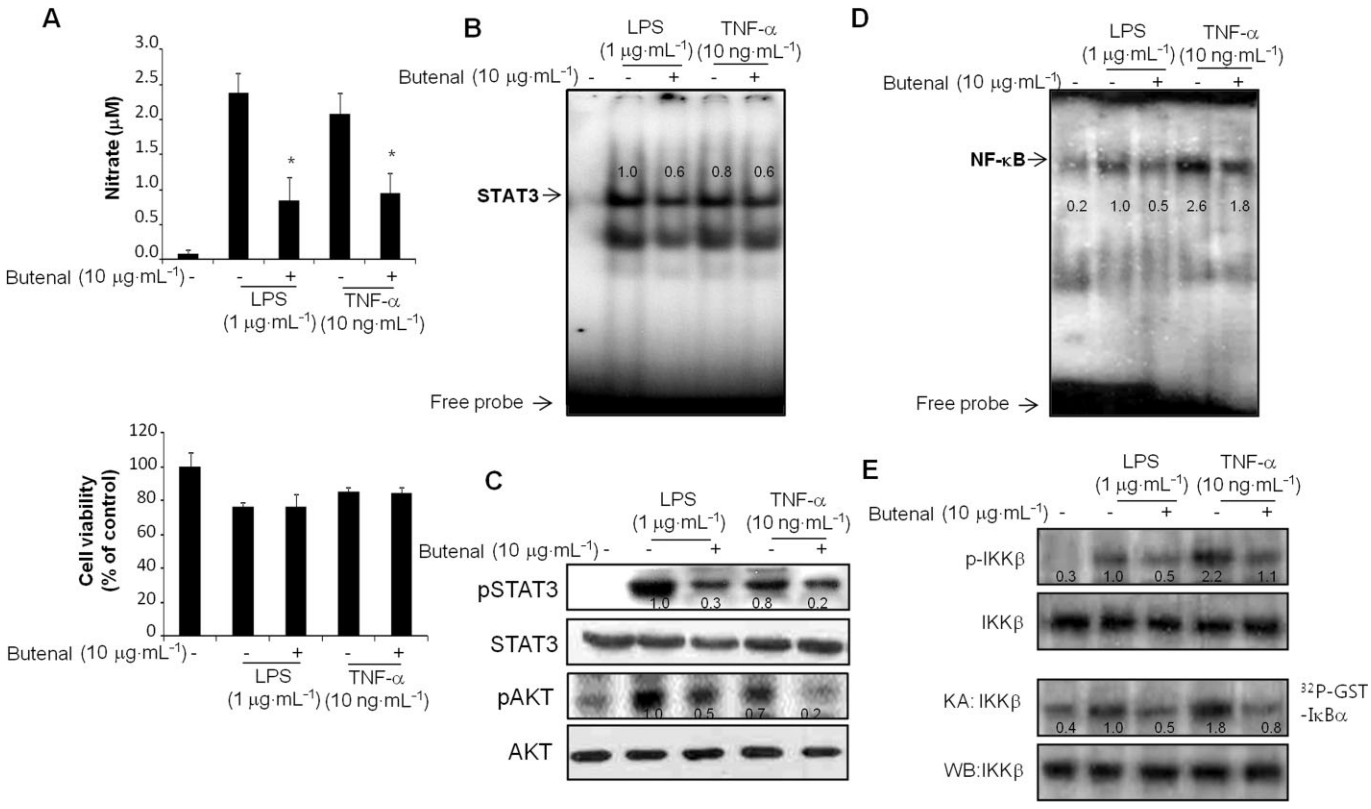

Figure 4

Inhibitory effect of (E)-2,4-bis(*p*-hydroxyphenyl)-2-butenal on LPS or TNF-α-induced NO generation, IKK/NF-κB activation in human synoviocytes. (A) NO generation (upper graph) and cell viability (lower graph), (B) DNA-binding activity of STAT3 and (C) phosphorylation of STAT3 and Akt, (D) DNA-binding activity of NF-κB and (E, upper panel) expression of IKKβ and their phosphorylated forms, as well as (E, lower panel) IKKβ activities were determined.

dose-dependent inhibition of the expression of iNOS and COX-2 (Figure 5F). In addition, in ankle joint tissues from CIA mice, (E)-2,4-bis(*p*-hydroxyphenyl)-2-butenal inhibited the activation of NF-κB DNA-binding activity (Figure 6A), the nuclear translocation of p50 and p65, and phosphorylation of IκB (Figure 6B) and of IKKβ (Figure 6C), as well as IKKβ kinase activity (Figure 6D). Moreover, it inhibited the collagen-induced STAT3 DNA-binding activity (Figure 6E) and phosphorylation of STAT3 (Figure 6F) as well as Akt (Figure 6F).

Direct binding of (E)-2,4-bis(p-hydroxyphenyl)-2-butenal with STAT3

There are several compounds that inhibit the STAT3 signal pathway through direct binding to STAT3 (Berman *et al.*, 2000; Yu *et al.*, 2002; Yang *et al.*, 2007; Lee *et al.*, 2011). We performed a computational docking experiment between (E)-2,4-bis(*p*-hydroxyphenyl)-2-butenal (Figure 7A) and STAT3 using Autodock VINA. (E)-2,4-bis(*p*-hydroxyphenyl)-2-butenal bound to the DNA-binding domain of STAT3 with –6.4 kca mol^{-1} affinity. Two hydrogen bonds were observed between the compound and the DNA-binding site of STAT3, more specifically with Asn^{567} and Arg^{335} (Figure 7B, C). These amino acid residues are essential for recognition of the DNA-binding element. Therefore, (E)-2,4-bis(*p*-hydroxyphenyl)-2-butenal may inhibit the kinase activity of STAT3 by blocking the binding of DNA to STAT3.

Discussion

In this study, we found that (E)-2,4-bis(*p*-hydroxyphenyl)-2-butenal inhibited LPS-induced ROS, NO and PGE_2 generation accompanied by a reduction in iNOS and COX-2 expression as well as IL-1β, TNF-α and IL-6 mRNA expression with decreased LPS-induced IKKβ/NF-κB and STAT3 activities in RAW 264.7 cells and in cultured human synoviocytes. *In vivo* animal studies revealed that (E)-2,4-bis(*p*-hydroxyphenyl)-2-butenal inhibited tissue swelling, fibrosis, and bone destruction in addition to iNOS and COX-2 expression, and NO release from spleen T-cells as well as inhibition of the IKKβ/NF-κB and STAT3 activities in a mouse model of arthritis. A docking model prediction showed that (E)-2,4-bis(*p*-hydroxyphenyl)-2-butenal may directly bind to STAT3, thereby blocking the activity of STAT3 as well as IKKβ/NF-κB activities. These data suggest that (E)-2,4-bis(*p*-hydroxyphenyl)-2-butenal could be a useful agent for the treatment of inflammatory diseases, such as rheumatoid arthritis.

Oxidative stress induced by ROS and NO contributes to the development of inflammatory diseases through the induction of IKK and NF-κB activity (Morgan and Liu, 2011).

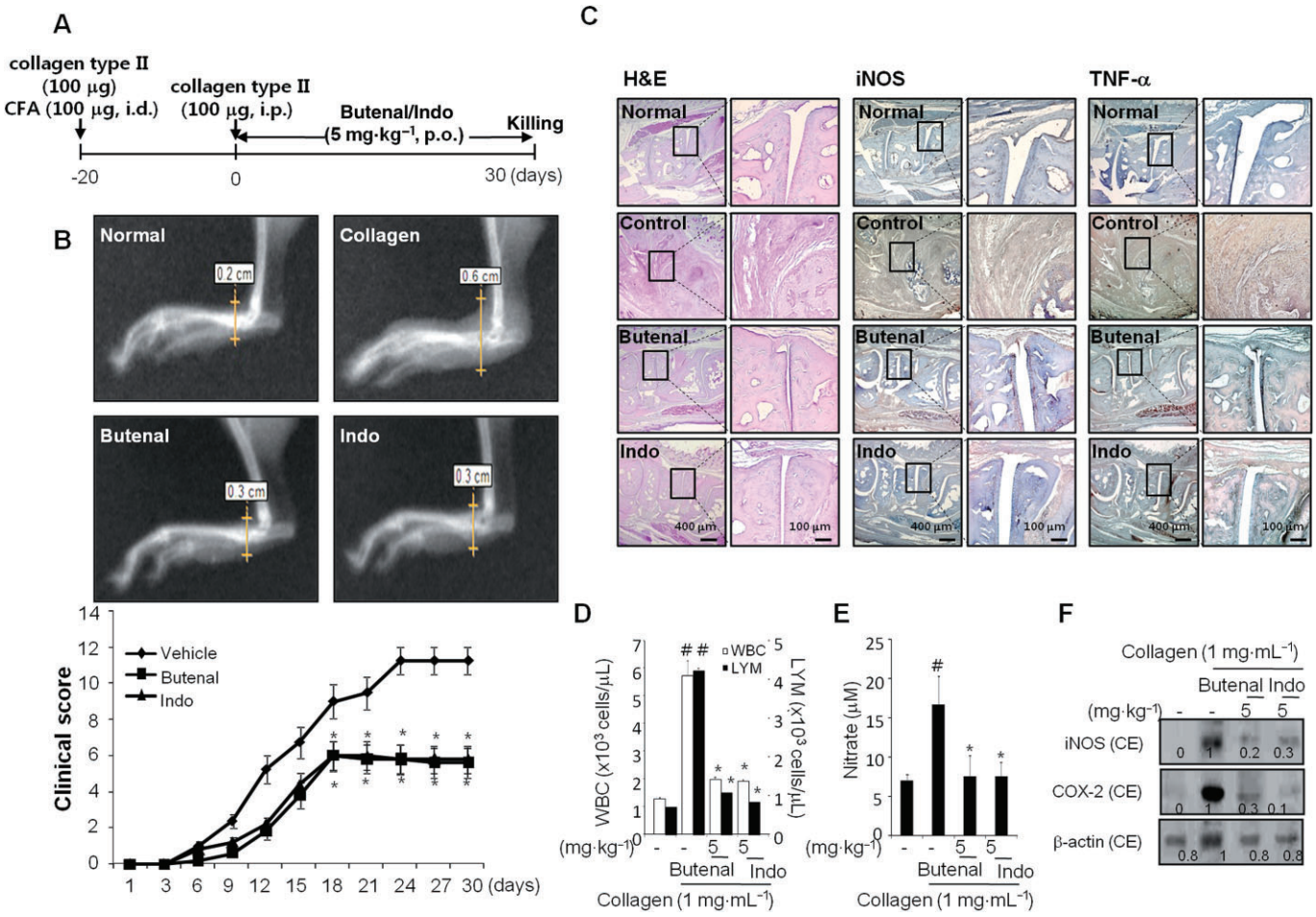

Figure 5

Inhibitory effect of (E)-2,4-bis(*p*-hydroxyphenyl)-2-butenal on the development of CIA in DBA1/J mice, compared with that of indomethacin (indo). (A) Experimental protocols. (B) A radiographic examination of hind paws revealed oedema in the paw after 30 days. Data shown are clinical scores from 10 mice. **P* < 0.05, significantly different from the collagen-treated group. (C) Haematoxylin & eosin (H&E) staining was used to evaluate (E)-2,4-bis(*p*-hydroxyphenyl)-2-butenal-mediated pathological changes in collagen-induced mice hind paw sections. Immunohistochemical assessment of expression levels of iNOS and TNF-α in mouse paw sections. (D) WBC and lymphocyte counts from the blood of CIA mice were measured by an HIE cell counter. (E) NO generation in spleen T-cells from CIA mice was measured by nitrate assay. (F) The expression of iNOS and COX-2 in mouse paw was detected by Western blotting. All values represent the means ± SD of 10 mice. $^{\#}P < 0.05$, significantly different from normal control group. **P* < 0.05 significantly different from the collagen-treated group.

Thus, antioxidants are expected to improve these disorders by anti-inflammatory responses. Several diets containing Maillard reaction products exhibit higher antioxidant activity (Valls-Bellés *et al.*, 2004; Yilmaz and Toledo, 2005; Yang *et al.*, 2011; Dhanik *et al.*, 2012). Similar to these products, (E)-2,4-bis(*p*-hydroxyphenyl)-2-butenal decreased LPS-induced NO and ROS in RAW 264.7 cells. Our studies also revealed the antioxidant effects of this compound in other *in vitro* systems such as astrocytes and microglia cells (Lee *et al.*, 2011). Many naturally occurring antioxidants such as those in turmeric, green tea and grapeseed have anti-inflammatory effects (Menon and Sudheer, 2007; Rosenbaum *et al.*, 2010). Considering these reports, the results from this study indicate that the antioxidant properties of (E)-2,4-bis(*p*-hydroxyphenyl)-2-butenal could be related to its anti-inflammatory activities. IKK/NF-κB regulates host inflammatory and immune response properties by increasing expression of specific cellular genes such as IL-1, IL-1β, IL-2, IL-6, IL-8 and TNF-α and pro-inflammatory genes encoding COX-2 and iNOS (Haefner, 2002). (E)-2,4-bis(*p*-hydroxyphenyl)-2-butenal inhibited LPS-induced IL-1β, TNF-α and IL-6 mRNA as well as iNOS and COX-2 expression through inhibition of NF-κB as well as IKKβ activity in both RAW 264.7 cells and human synoviocytes. Our present data is on agreement with our earlier finding that (E)-2,4-bis(*p*-hydroxyphenyl)-2-butenal showed anti-amyloidogenic effect and ameliorated memory dysfunction in Alzheimer's disease transgenic mice model through inhibition of oxidative and neuroinflammatory responses via inactivation of NF-κB pathway (Jin *et al.*, 2013). Thus, inhibition of the IKKβ/NF-κB signal pathway by reduction of oxidants may be involved in the anti-inflammatory effects of (E)-2,4-bis(*p*-hydroxyphenyl)-2-butenal.

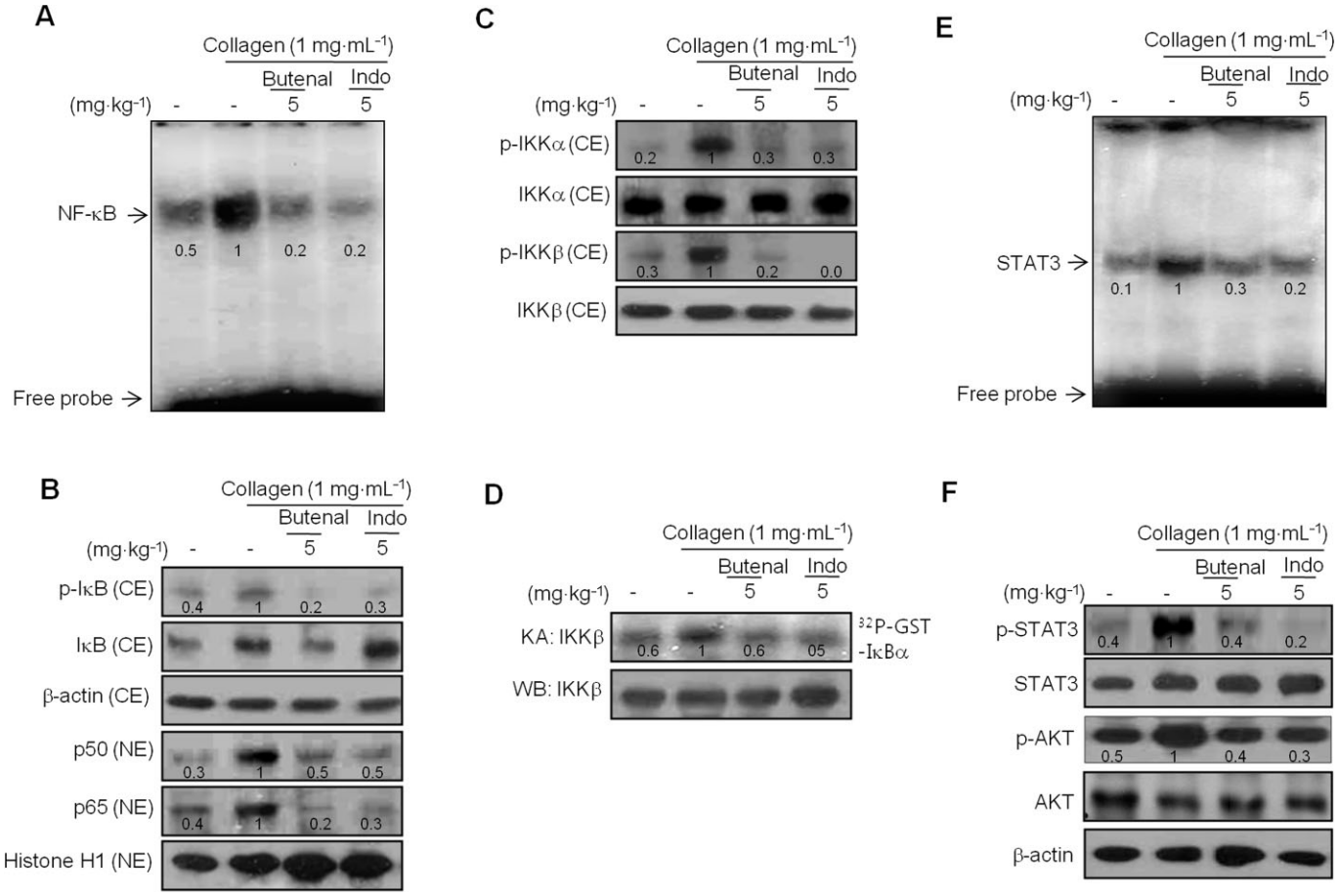

Figure 6

Inhibitory effect of (E)-2,4-bis(*p*-hydroxyphenyl)-2-butenal on IKK/NF-κB and STAT3 activation in arthritic tissues from mice with CIA, compared with that of indomethacin (indo). The DNA-binding activity of (A) NF-κB and (E) STAT3 was determined by EMSA. (B) The nuclear translocation of p50 and p65 and the degradation of IκB were detected by Western blotting. The total and phosphorylated protein levels of (C) IKKα, IKKβ and (F) STAT3 and Akt were determined (D). The quantification of band intensities from three mice indicated by the values under each band indicates the fold difference (average) from the untreated control group.

STAT3 is another important redox transcription factor that is involved in inflammation and immune responses in arthritis. It is also crucial for regulation of the expression of inflammatory mediators, such as iNOS, COX-2, IL-6 and IL-1β (Lo *et al.*, 2005; Nowell *et al.*, 2009). Several antioxidants such as moxibustion compounds may have anti-inflammatory and anti-arthritis effects by preventing STAT3 activation (Yang *et al.*, 2007). Nowell *et al.* (2009) reported that STAT3 is critical for IL-6-induced synovial infiltration in inflammatory arthritis. Compatible with these findings, the anti-inflammatory and anti-arthritis effects of (E)-2,4-bis(*p*-hydroxyphenyl)-2-butenal were correlated with the inhibition of STAT3 activity *in vitro* and *in vivo*. Several reports have suggested that STAT3 could interact with NF-κB (Yu *et al.*, 2002; Hagihara *et al.*, 2005; Kim *et al.*, 2011). In the study of the connection between NF-κB and STAT3 pathway, our findings also showed that depletion of STAT3 using an inhibitor or siRNA reversed the inhibitory effect of (E)-2,4-bis(*p*-hydroxyphenyl)-2-butenal on NO generation and NF-κB activity and decreased the mRNA levels of pro-inflammatory cytokines. Taken together, the antioxidant and anti-inflammatory effects of (E)-2,4-bis(*p*-hydroxyphenyl)-2-butenal could be related to the cooperative down-regulation of IKK/NF-κB and STAT3 and Akt pathways. They also show the importance of the STAT3 pathway in the anti-inflammatory effect of this compound.

As demonstrated by its anti-inflammatory effects *in vitro*, the present study showed that (E)-2,4-bis(*p*-hydroxyphenyl)-2-butenal treatment decreased iNOS and COX-2 expression as well as NF-κB DNA binding, IKKβ and STAT3 activities in the ankle joints of CIA mice. We also found that this compound inhibited the production of NO in spleen cytotoxic T-cells (may be $CD8^+$ cells). In the synovium of patients with active rheumatoid arthritis, activation of the NF-κB and STAT3 pathway induces a variety of genes that contribute to the inflammatory response, such as those for iNOS and IL-6, which recruit immune cells to the inflamed pannus (Tomita *et al.*, 2000; de Hooge *et al.*, 2004). In this study, (E)-2,4-bis(*p*-hydroxyphenyl)-2-butenal-treated mice showed decreased fibrosis and bone erosion in arthritic joints, compared with that from untreated CIA mice. (E)-2,4-bis(*p*-hydroxyphenyl)-2-butenal also suppressed the numbers of circulating WBC,

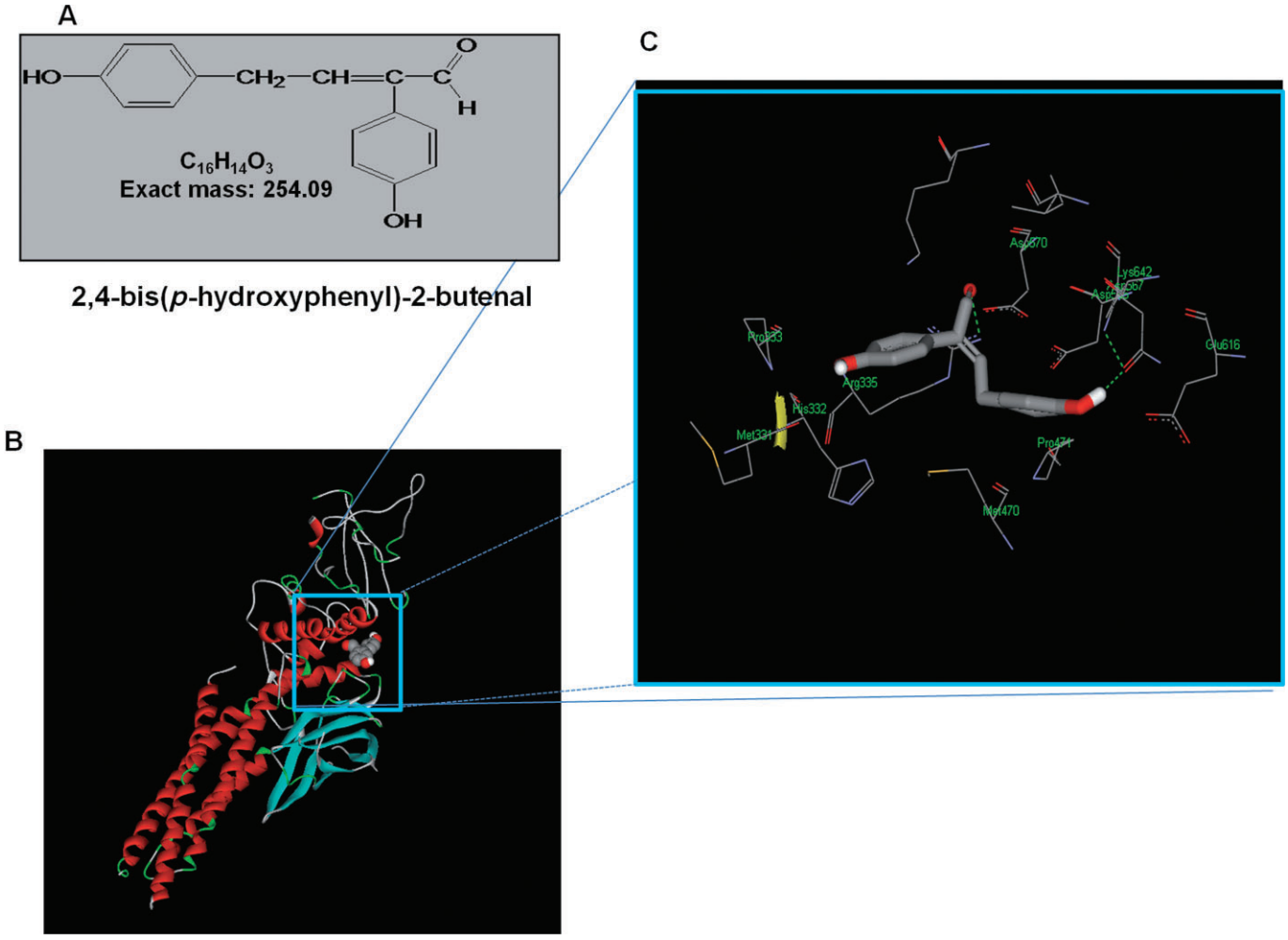

Figure 7

Modelling study of the binding of (E)-2,4-bis(*p*-hydroxyphenyl)-2-butenal binding to IKKβ protein. (A) Chemical structure of (E)-2,4-bis(*p*-hydroxyphenyl)-2-butenal. (B) Three-dimensional modelling of (E)-2,4-bis(*p*-hydroxyphenyl)-2-butenal binding within the DNA-binding domain of STAT3. The amino acids of STAT3 involved in the hydrogen bonding interactions (in box) with (E)-2,4-bis(*p*-hydroxyphenyl)-2-butenal represented by sticks, and the additional portions of the protein are shown as ribbons. (C) The two-dimensional ligand interaction diagram of (E)-2,4-bis(*p*-hydroxyphenyl)-2-butenal and STAT3. Amino acid residues of STAT3 involved in the hydrogen bonding interactions are shown.

an indicator of inflammation or infection in collagen-induced mice (Awolfson, 2009). The effective dose of (E)-2,4-bis(*p*-hydroxyphenyl)-2-butenal (5 mg·kg^{-1}) used in the CIA study was comparable to that of indomethacin (5 mg·kg^{-1}), a classic anti-inflammatory drug.

Although the anti-inflammatory and anti-arthritis effects could be associated with the inhibition of the NF-κB/IKKβ and STAT3/Akt pathways, the critical targets are not clear. It is well known that the activity of NF-κB is primarily regulated by STAT3 (Yu *et al.*, 2002; Yang *et al.*, 2007; Kim *et al.*, 2011) and the inhibition of STAT3 is now widely recognized as a valid strategy for combating inflammatory diseases. Many research groups have reported that target proteins, STAT3, often form hydrogen bonds with a hydroxyl group of low MW compounds, resulting in the inhibition of its activity (Berman *et al.*, 2000; Lee *et al.*, 2011). Our docking model shows that (E)-2,4-bis(*p*-hydroxyphenyl)-2-butenal may bind to the hydroxyl group of the DNA-binding site of STAT3. Therefore, (E)-2,4-bis(*p*-hydroxyphenyl)-2-butenal could interfere with STAT3, thereby resulting in blocking of NF-κB-mediated signals. Very similar to our findings, Zhu and Jing (2007) have demonstrated that T40214 binds competitively to the DNA-binding site of STAT3, thereby impairing the activation of STAT3. Taken together, the antioxidant and anti-inflammatory compound (E)-2,4-bis(*p*-hydroxyphenyl)-2-butenal, interfered with STAT3-mediated NF-κB/Akt signals, thus inducing an anti-arthritic effect *in vivo*. These data indicate that (E)-2,4-bis(*p*-hydroxyphenyl)-2-butenal may be potentially beneficial in preventing inflammatory diseases such as rheumatoid arthritis.

Acknowledgements

This work was supported by the National Research Foundation of Korea (NRF) grant funded by the Korea government

(MSIP) (No. MRC,2008-0062275), and by the Ministry of Trade, Industry, & Energy (MOTIE, 141526993) through the fostering project of Osong Academy-Industry Convergence (BAIO).

Conflict of interest

The authors have no conflict of interest to declare.

References

Aeschbacher HU (1990). Anticarcinogenic effect of browning reaction products. In: Finot PA, Aeschbacher HU, Hurrell RF, Liardon R (eds). The Maillard Reaction in Food Processing, Human Nutrition and Physiology: Birkhauser: Basel, Switzerland, pp. 335–347.

Awolfson AB (2009). Harwood-Nuss' Clinical Practice of Emergency Medicine. Lippincott Williams & Wilkins: Baltimore, MD, pp. 375–376.

Ban JO, Oh JH, Hwang BY, Moon DC, Jeong HS, Lee S *et al.* (2009). Inflexinol inhibits colon cancer cell growth through inhibition of nuclear factor-kappaB activity via direct interaction with p50. Mol Cancer Ther 8: 1613–1624.

Berman HM, Westbrook J, Feng Z, Gilliland G, Bhat TN, Weissig H *et al.* (2000). The protein data bank. Nucleic Acids Res 28: 235–242.

Dhanik A, McMurray JS, Kavraki LE (2012). Binding modes of peptidomimetics designed to inhibit STAT3. PLoS ONE 7: e51603.

Grivennikov SI, Karin M (2010). Inflammation and oncogenesis: a vicious connection. Curr Opin Genet Dev 20: 65–71.

Haefner B (2002). NF-κB: arresting a major culprit in cancer. Drug Discov Today 7: 653–663.

Hagihara K, Nishikawa T, Sugamata Y, Song J, Isobe T, Taga T *et al.* (2005). Essential role of STAT3 in cytokine-driven NF-kappaB-mediated serum amyloid A gene expression. Genes Cells 10: 1051–1063.

de Hooge AS, van de Loo FA, Koenders MI, Bennink MB, Arntz OJ, Kolbe T *et al.* (2004). Local activation of STAT-1 and STAT-3 in the inflamed synovium during zymosan-induced arthritis: exacerbation of joint inflammation in STAT-1 gene-knockout mice. Arthritis Rheum 50: 2014–2023.

Hwang IG, Kim HY, Woo KS, Hong JT, Hwang BY, Jung JK *et al.* (2011). Isolation and characterisation of an a-glucosidase inhibitory substance from fructose–tyrosine Maillard reaction products. Food Chem 127: 122–126.

Jin P, Kim JA, Choi DY, Lee YJ, Jung HS, Hong JT (2013). Anti-inflammatory and anti-amyloidogenic effects of a small molecule, 2,4-bis(*p*-hydroxyphenyl)-2-butenal in Tg2576 Alzheimer's disease mice model. J Neuroinflammation 5: 10–12.

Kilkenny C, Browne W, Cuthill IC, Emerson M, Altman DG (2010). Animal research: Reporting *in vivo* experiments: the ARRIVE guidelines. Br J Pharmacol 160: 1577–1579.

Kim JA, Yun HM, Jin P, Lee HP, Han JY, Udumula V *et al.* (2013). Inhibitory effect of a 2,4-bis(4-hydroxyphenyl)but-2-enal diacetate on neuro-inflammatory reactions via inhibition of STAT1 and STAT3 activation in cultured astrocytes and microglial BV-2 cells. Neuropharmacology 79C: 476–487.

Kim MM, Kim SK (2010). Effect of phloroglucinol on oxidative stress and inflammation. Food Chem Toxicol 48: 2925–2933.

Kim SK, Park KY, Yoon WC, Park SH, Park KK, Yoo DH *et al.* (2011). Melittin enhances apoptosis through suppression of IL-6/sIL-6R complex-induced NF-κB and STAT3 activation and Bcl-2 expression for human fibroblast-like synoviocytes in rheumatoid arthritis. Joint Bone Spine 78: 471–477.

Kim YJ, Kim YA, Yokozawa T (2010). Attenuation of oxidative stress and inflammation by gravinol in high glucose-exposed renal tubular epithelial cells. Toxicology 270: 106–111.

Kowluru RA, Kanwar M (2007). Effects of curcumin on retinal oxidative stress and inflammation in diabetes. Nutr Metab (Lond) 16: 4–8.

Lee YJ, Choi DY, Choi IS, Han JY, Jeong HS, Han SB *et al.* (2011). Inhibitory effect of a tyrosine-fructose Maillard reaction product, 2,4-bis(*p*-hydroxyphenyl)-2-butenal on amyloid-β generation and inflammatory reactions via inhibition of NF-κB and STAT3 activation in cultured astrocytes and microglial BV-2 cells. J Neuroinflammation 7: 8–132.

Lo HW, Hsu SC, Ali-Seyed M, Gunduz M, Xia W, Wei Y *et al.* (2005). Nuclear interaction of EGFR and STAT3 in the activation of the iNOS/NO pathway. Cancer Cell 7: 575–589.

Ma Q (2010). Transcriptional responses to oxidative stress: pathological and toxicological implications. Pharmacol Ther 125: 376–393.

McGrath J, Drummond G, McLachlan E, Kilkenny C, Wainwright C (2010). Guidelines for reporting experiments involving animals: the ARRIVE guidelines. Br J Pharmacol 160: 1573–1576.

Menon VP, Sudheer AR (2007). Antioxidant and anti-inflammatory properties of curcumin. Adv Exp Med Biol 595: 105–125.

Monti SM, Ritieni A, Graziani G, Randazzo G, Mannina L, Segre AL *et al.* (1999). LC/MS analysis and antioxidative efficiency of Maillard reaction products from a lactose-lysine model system. J Agric Food Chem 47: 1506–1513.

Morgan MJ, Liu ZG (2011). Crosstalk of reactive oxygen species and NF-κB signaling. Cell Res 21: 103–115.

Nah SS, Won HJ, Ha E, Kang I, Cho HY, Hur SJ *et al.* (2010). Epidermal growth factor increases prostaglandin E2 production via ERK1/2 MAPK and NF-kappaB pathway in fibroblast like synoviocytes from patients with rheumatoid arthritis. Rheumatol Int 30: 443–449.

Nowell MA, Williams AS, Carty SA, Scheller J, Hayes AJ, Jones GW *et al.* (2009). Therapeutic targeting of IL-6 trans signaling counteracts STAT3 control of experimental inflammatory arthritis. J Immunol 182: 613–622.

Okamoto H, Yoshio T, Kaneko H, Yamanaka H (2010). Inhibition of NF-kappaB signaling by fasudil as a potential therapeutic strategy for rheumatoid arthritis. Arthritis Rheum 62: 82–92.

Peng Q, Wei Z, Lau BH (2000). Pycnogenol inhibits tumor necrosis factor-alpha-induced nuclear factor kappa B activation and adhesion molecule expression in human vascular endothelial cells. Cell Mol Life Sci 57: 834–841.

Phillips DC, Dias HK, Kitas GD, Griffiths HR (2010). Aberrant reactive oxygen and nitrogen species generation in rheumatoid arthritis (RA): causes and consequences for immune function, cell survival, and therapeutic intervention. Antioxid Redox Signal 12: 743–785.

Ren Z, Mao X, Mertens C, Krishnaraj R, Qin J, Mandal PK *et al*. (2008). Crystal structure of unphosphorylated STAT3 core fragment. Biochem Biophys Res Commun 374: 1–5

Rosenbaum CC, O'Mathúna DP, Chavez M, Shields K (2010). Antioxidants and antiinflammatory dietary supplements for osteoarthritis and rheumatoid arthritis. Altern Ther Health Med 16: 32–40.

Tomita T, Takano H, Tomita N, Morishita R, Kaneko M, Shi K *et al*. (2000). Transcription factor decoy for NF-κB inhibits cytokine and adhesion molecule expressions in synovial cells derived from rheumatoid arthritis. Rheumatology 39: 749–757.

Trott O, Olson AJ (2010). AutoDock Vina: improving the speed and accuracy of docking with a new scoring function, efficient optimization, and multithreading. J Comput Chem 31: 455–461.

Valls-Bellés V, Torres MC, Muñiz P, Boix L, González-Sanjose M Codoñer-Franch P (2004). The protective effect of melanoidins in adriamycin-induced oxidative stress in rat isolated hepatocytes. J Sci Food Agric 84: 1701–1707.

Yang SH, Khadka DB, Cho SH, Ju HK, Lee KY, Han HJ *et al*. (2011). Virtual screening and synthesis of quinazolines as novel JAK2 inhibitors. Bioorg Med Chem 19: 968–977.

Yang X, Li JS, Yang SQ, Zhang XX, Zhang TS, Zhou HY *et al*. (2007). Influence of moxibustion on JAK-STAT signal transduction pathways of synovial cells in rheumatoid arthritis rabbits. Zhen Ci Yan Jiu 32: 75–82.

Yen GC, Tsai LC, Lii JD (1992). Antimutagenic effect of Maillard browning products obtained from amino acids and sugars. Food Chem Toxicol 30: 127–132.

Yilmaz Y, Toledo R (2005). Antioxidant activity of water-soluble Maillard reaction products. Food Chem 93: 273–278.

Yu Z, Zhang W, Kone BC (2002). Signal transducers and activators of transcription 3 (STAT3) inhibits transcription of the inducible nitric oxide synthase gene by interacting with nuclear factor kappaB. Biochem J 367: 97–105.

Zhu Q, Jing N (2007). Computational study on mechanism of G-quartet oligonucleotide T40214 selectively targeting Stat3. J Comput Aided Mol Des 21: 641–648.